Journal of Membrane Science Letters 3 (2023) 100052

Contents lists available at ScienceDirect

Journal of Membrane Science Letters

journal homepage: www.elsevier.com/locate/memlet

Opportunities for isoporous membranes in the manufacture of genomic medicines

Ke Meng [b], Thomas F. Johnson [b], Alberto Alvarez-Fernandez [a], Stefan Guldin [a], Daniel G. Bracewell [b,*]

[a] Department of Chemical Engineering, University College London, Torrington Place, London, WC1E 7HB, UK
[b] Department of Biochemical Engineering, Gower Street, University College London, London, WC1E 6BT, UK

ARTICLE INFO

Keywords:
Isoporous membranes
Genomic medicine
Bio-separation
Ultrafiltration
Block copolymer membranes

ABSTRACT

Viral and non-viral vectors have revolutionised in the last 5 years the approaches to tackling pandemics, cancers and genetic diseases. The intrinsic properties of these vectors present new separation challenges to their manufacture in terms of both the process-related impurities to be removed and the complex labile nature of the target products. These characteristics make them susceptible to heterogeneity and the formation of product-related impurities.

Conventional polyethersulfone membrane filters used for sterile filtration and ultrafiltration of viral vectors and lipid nanoparticles can display limited selectivity and cause product losses. To address these challenges, novel membrane materials and fabrication techniques to overcome the boundary of selectivity-permeability performance have become of interest. Isoporous membranes with well-defined pore size and pore dispersity at the nano-scale show promising separation performance but have only been demonstrated at small scales to date.

This review summarises the decision process for the development of new membrane candidates for vector manufacturing in genomic medicine, including membranes fabricated by lithography, track-etched membranes, anodic aluminium oxide (AAO) membranes and self-assembled block copolymer membranes. By comparing these membranes to existing commercially available products, the possible advantages presented by novel materials and fabrication approaches are identified.

1. An introduction to vectors for genomic medicine delivery

1.1. Viral vector delivery

The rise in popularity of genomic medicines for clinical applications has driven the need to manufacture a variety of viral vectors. These vectors include adeno-associated virus (AAV), adenovirus (AV), and lentivirus (LV). When compared to therapeutic proteins, the currently dominant class of biological products for therapeutic use, these products are a) more complex and often carry a genetic payload that must be correctly packaged within a capsid or lipid structure composed of multiple components and b) larger in size by around one order of magnitude in diameter. Consequently, these characteristics present new separation challenges (Srivastava et al., 2021, Segura et al., 2011).

1.1.1. Viral vector separation challenges due to complexity

The best known of these is the separation of empty vs full capsids, i.e., the separation of viruses with and without their genetic payload. This is a problem particularly prevalent in AAV. It is likely as understanding of the critical quality attributes of these complex vectors increase then other factors will need to be taken into consideration, such as the extent of glycosylation on the vector surface (Ozdilek and Avci, 2022).

1.1.2. Viral vector separation challenges due to size

As complex biological products are synthesised in mammalian cells, concerns about bacterial and viral contamination must be addressed. Sterile filtration is therefore a critical requirement of the majority of processes (Singh and Heldt, 2022). When compared to therapeutic proteins,

Abbreviations: AAO, Anodic aluminium oxide; BCM, Block copolymer membrane; AAV, Adeno-associated virus; LNPs, Lipid nanoparticles; BSA, Bovine serum albumin; PEO, Polyethylene oxide; HRV, Human Rhinovirus; LNTs, Lipid Nanotubes; BHb, Bovine haemoglobin; IgG, Immunoglobulin G; HGH, Human growth hormone; NIPS, Non-solvent-induced phase separation; CNTs, Carbon nanotubes; PC, Polycarbonate; PET, Poly(ethylene terephthalate); NIPS, Non-solvent Induced Phase Separation; PDMS, Polydimethylsiloxane; PEGDA, Poly(ethylene glycol) diacrylate; PVP, Polyvinylpyrrolidone; PI, Polyimide; PP, Polypropylene; PVDF, Polyvinylidene difluoride.

* Corresponding author at: Department of Biochemical Engineering, Gower Street, University College London, London, WC1E 6BT, UK.
E-mail address: d.bracewell@ucl.ac.uk (D.G. Bracewell).

https://doi.org/10.1016/j.memlet.2023.100052
Received 14 May 2023; Received in revised form 17 June 2023; Accepted 19 June 2023

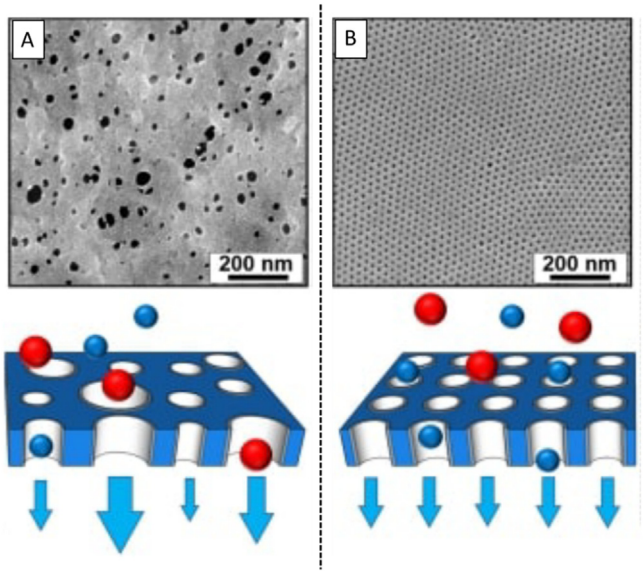

Fig. 1. (a) SEM image of a commercial ultrafiltration membrane prepared by non-solvent induced phase separation (NIPs) (b) SEM image of a block copolymer membrane. The schematic models represent the filtration process to separate particles by the size difference. Red and blue particles are solutes with different radii. The figure is reprinted with permission from (Zhang et al., 2018). Copyright 2018 Nature.

the larger size of viruses approaching that of bacterial cells raises the level of difficulty in achieving size-based separation using membranes in ensuring successful sterile filtration.

1.2. Lipid nanoparticle delivery and associated separation challenges

An alternative delivery vehicle for genomic medicines is lipid nanoparticles (LNPs), as exemplified by mRNA vaccines in prophylactic applications (Samaridou et al., 2020) . The modality also has the potential for a broad variety of therapeutic uses. The separation challenges have much in common with viral vectors when compared to proteins. They too are relatively complex and large, therefore exhibiting common challenges in areas such as sterile filtration.

2. Technical challenges in the purification of vectors for genomic medicine

Sterile filtration and ultrafiltration membranes are widely implemented in the downstream separation of viral vectors and LNPs for the recovery, purification, concentration and formulation of the products. As shown in Fig. 1a, commercially available polymeric membranes offer good permeability but have poor selectivity, due to their wide pore size distribution and interconnected pore channels (Yang and Zhang, 2018). Conventional materials and fabrication techniques cannot achieve any greater control of pore size and dispersity. However, advances in nanomaterials and fabrication techniques have enabled improved ordering of pore size and dispersity as displayed in Fig. 1b. Examples include block copolymer membranes (Qiu et al., 2013, Dorin et al., 2014, Yang et al., 2006) and anodic aluminium oxide membranes (Sharma and Bracewell, 2019, Osmanbeyoglu et al., 2009, Jeon et al., 2014).

This category of membranes having ordered, dense, and uniform pores with straight channels are called 'isoporous membranes' and are designed to achieve precise solute rejection based on size discrimination. These membranes fabricated by organic and inorganic materials exhibit a range of mechanical flexibility, stability and anti-fouling properties (Phillip et al., 2010). This review begins with the main challenges and initiatives in the downstream separation of vectors used in genomic medicine. Isoporous membrane technology for sterile filtration and ultrafiltration is evaluated and several candidates are compared. This includes lithography, track etched membranes, anodic aluminium oxide membranes and block copolymer membranes. The fabrication techniques for making these membranes are summarised and the potential of this technology for bioprocessing purposes is discussed.

2.1. Viral vectors - separation of empty versus full AAV capsids

Mainstream viral vectors such as adeno-associated virus, adenovirus, lentivirus and herpes simplex virus have different features including charge, size, gene payload and immunogenicity. Among them, AAV has been recognised as one of the most popular vectors for delivery (Lundstrom, 2003).

One of the key challenges for manufacturing AAV is to separate full capsids from the empty and non-infective capsids in different serotypes to meet requirements of purity, efficacy and safety (Segura et al., 2011). The full, empty and non-infective particles have a minimal difference in surface chemistry, size and charge (Srivastava et al., 2021). Therefore, column-based separation techniques such as affinity, size exclusion and ionic exchange chromatography are not always compatible and overlap when eluted, which leads to considerable product loss and low yield. Moreover, harsh column elution conditions, extreme pH and high salts could damage viral particles and cause further loss (Srivastava et al., 2021).

As shown in Fig 2, chromatography columns are still the most widely-used and well-established techniques in the downstream processing for viral vector manufacturing, which attributes to their excellent scalability, stability and reproducibility. Another method based on the density difference between full and empty capsids widely used in the laboratory is CsCl density gradient ultracentrifugation. However, this method is expensive, laborious, non-scalable and sensitive to operating conditions, which limits its application to the production scales (Segura et al., 2011).

2.2. Sterile filtration for the recovery of viral vectors and lipid nanoparticles (LNPs)

Sterile filtration, within the range of microfiltration (MF), is the most expensive unit operation in the downstream process of AAV production (Srivastava et al., 2021). Sterile filtration operates in the normal flow filtration mode (commonly referred to as dead-end) and removes impurities based on size exclusion. Ideally the product of interest passes through the filter and any larger wanted components are rejected. However, when viral particles travel through the membrane surface and the porous structure, they are likely to aggregate due to shear stress and adsorb to the polymer surface, which results in product yield loss (Srivastava et al., 2021). Another struggle is to find a sterile filter with a suitable pore size for these large particles. Membranes with rated 0.2 μm and 0.45 μm nominal pore sizes are most commonly used for a sterilising grade filtration process. However, whilst this is suitable for conventional products such as monoclonal antibodies, larger viral vectors present filtration challenges.

To formulate LNPs commercially, an extrusion step is commonly adopted by passing feed through single or multiple isoporous membrane filters, e.g. polycarbonate track-etched membranes (Carugo et al., 2016). This process can produce LNPs with customised average sizes and various size distributions (polydispersity index reported from 0.1 to 0.4) (Ong et al., 2016, Jousma et al., 1987, Maurer et al., 2001). However, PC track-etched membranes are only available in lab scales and tend to foul quickly when handling polydisperse LNPs, which severely impacts productivity (Jousma et al., 1987).

2.3. Ultrafiltration for the purification of viral vectors

Ultrafiltration is an important unit operation and is usually implemented multiple times in the downstream bioprocessing, such as

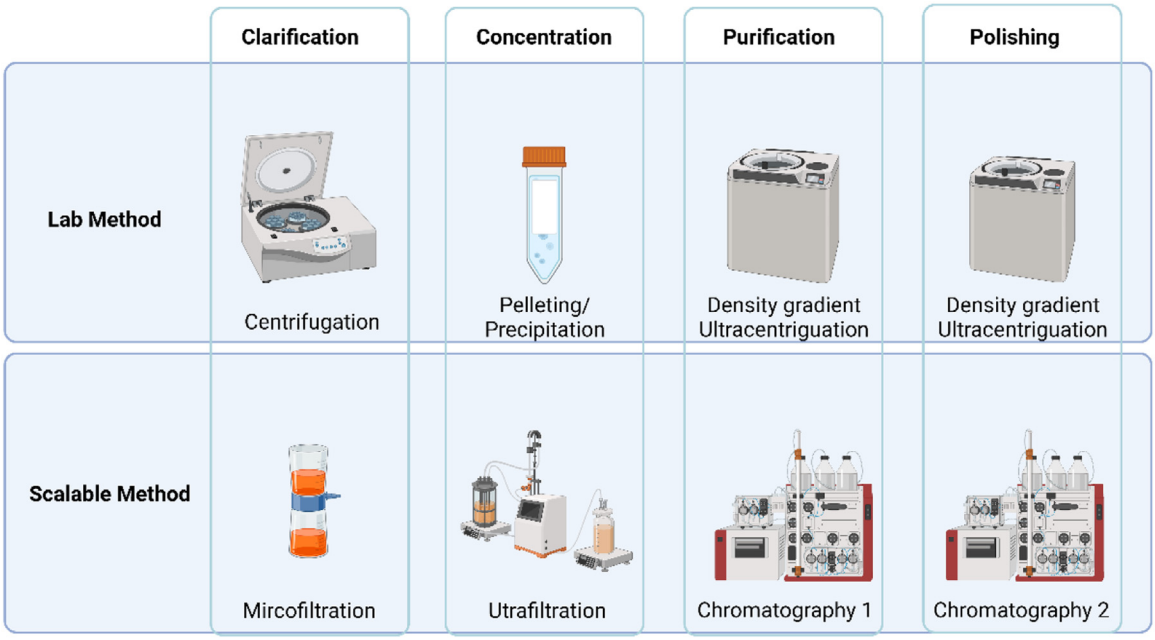

Fig. 2. Strategy for viral vectors downstream purification at laboratory and production scales. This figure is adapted from (Segura et al., 2011) and was created using Biorender (Aoki and BIORENDER, 2017).

buffer exchange, protein purification, concentration and formulation (Jungbauer, 2013). Compared with sterile filtration, ultrafiltration membranes normally have finer pores at the skin layer for achieving good rejection, but this feature leads to low permeability and therefore prolonged processing times (Vishali and Kavitha, 2021). Moreover, large biological particles such as viral vectors and LNPs show significant diffusion limitations for pressure-driven filtration processes, which causes noticeable concentration polarization. At a high driving pressure, the phenomenon becomes more severe and further increases processing time. Therefore, ultrafiltration normally operates in tangential flow filtration mode to minimise concentration polarization and reduce fouling (Sablani et al., 2001). Although increasing the filtration area can shorten the processing time, it proportionally contributes to material costs. The selectivity-permeability performance and anti-fouling properties are key characteristics for ultrafiltration purposes[14]. Ultrafiltration membranes with these characteristics are demanding in the bioprocessing industry.

2.4. Membrane design: selective/permeability trade-offs

The design of a new membrane must consider selectivity, permeability, anti-fouling resistance (capacity), and physical/chemical stability (Phillip et al., 2011). Among them, selectivity and permeability are the two most critical parameters, and their relationship is always a trade-off. The reason is that the selectivity-permeability performance of commercial membranes is limited by the characteristics of conventional membrane materials and fabrication techniques.

The selectivity versus permeability trade-off as displayed in Fig. 3a for gas separation membranes was first summarised by Robeson in 1991 (Sablani et al., 2001) and then revisited in 2008, widely referred to the 'Robeson upper-bound plot' (Robeson, 2008). The shifting of the upper bound from 1991 to 2008 implies that the advancement of new materials and fabrication techniques have contributed to improving membrane performance. Similarly, the 'Robeson plot' for ultrafiltration membranes in Fig. 3b was first summarised by Mehta and Zydney in 2005, who used bovine serum albumin (BSA) as the model solute (Mehta and Zydney, 2005). Towards the boundary, novel isoporous membranes fabricated by new materials or techniques that could exceed the trade-off have been reported, such as block copolymer membranes (Radjabian and Abetz, 2015, Wang et al., 2020), and porous anodic aluminium membranes (Lee and Mattia, 2013).

3. Isoporous membranes, their fabrication methods and applications in bioprocessing

3.1. Isoporous membranes importance

The Robeson plot maps the selectivity-permeability performance boundary of current membranes. It gives the directions for seeking the ideal membrane in a two-dimensional coordinate, stability and anti-fouling features. As is shown in Fig. 4, membranes used in bioseparations are mainly microfiltration (MF) and ultrafiltration (UF). The solute transport mechanism is determined by size exclusion, which means that the solute is either travelling through or rejected by the membrane surface and inner pore channel (Werber et al., 2016). Even with the same nominal pore size, membranes with different pore size distributions at the surface tend to exhibit differing selectivities.

Conventional MF and UF membranes that have been widely used in industry, such as polyethersulfone (PES), are made by non-solvent induced phase separation (NIPs) process (Loeb and Sourirajan, 1963). This method obtains membranes with an asymmetric structure: a thin selective surface layer and a thick macroporous sponge-like supporting layer. However, it results in a non-uniform pore size distribution at the surface and tortuous interconnected pore channels that follow a gamma function distribution as seen in Fig. 5a. The high percentage of large pores allows a wide range of particles to travel through the membranes, which restricts rejection capability.

Examples approaching ideal isoporous membranes are polycarbonate track-etched and anodic aluminium oxide (AAO) membranes, shown in Fig. 5b. The pore size distribution shows a narrow log-normal distribution function and performs a sharper selectivity than the membrane in the first column. However, the former has low pore density which leads to poor permeability. Although the latter has high porosity, the separation thickness is a few hundreds of microns in order to retain mechanical strength, which results in poor permeability. Moreover, both candidates have limited scale-up potential and are only available at analytical scales.

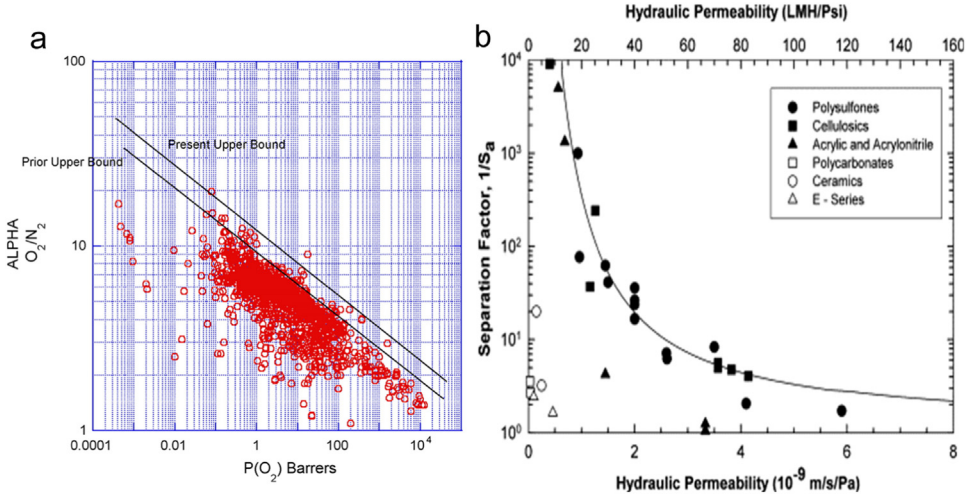

Fig. 3. (a) Upper boundary for O2/N2 separation in 1991 and 2008. The figure is reprinted with permission from (Robeson, 2008). Copyright 2008 Elsevier. (b) The selectivity versus permeability plot for ultrafiltration membranes using BSA ($R_h \approx 4$ nm) as the benchmark solute. The figure is reprinted with permission from (Mehta and Zydney, 2005). Copyright 2005 Elsevier.

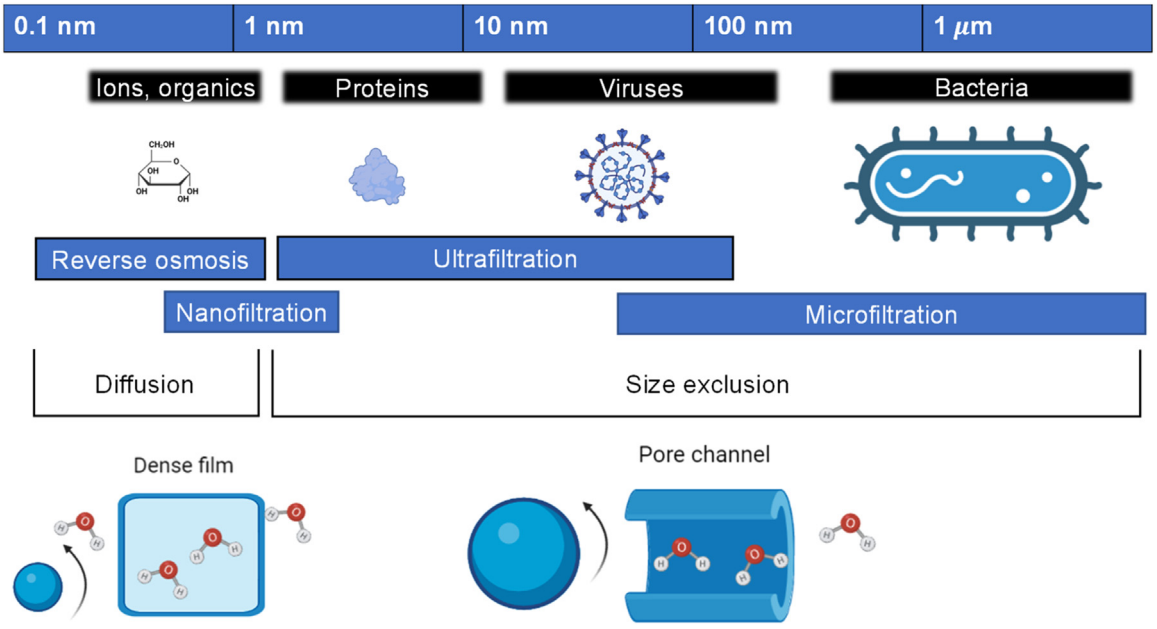

Fig. 4. The solute transport mechanism is dominated by size exclusion in microfiltration and ultrafiltration, and dominated by solution diffusion in reverse osmosis and forward osmosis. In nanofiltration, the solute transport mechanism combines size exclusion and solution diffusion. This figure is adapted from (Werber et al., 2016) and is created by Biorender (Aoki and BIORENDER, 2017).

An ideal isoporous membrane as displayed in Fig. 5c should have a uniform pore size distribution, high porosity, straight pore channels, and be able to give high permeability. The surface pore size distribution is a delta function and is expected to achieve precise rejection. This brings a proposed filtration model with a composited asymmetric structure: a top thin layer with uniform pore size, straight pore channels and high pore density to achieve good selectivity and permeability performance in addition to a rigid bottom layer with macroporous 'sponge-like' structure to provide mechanical support. New membrane concepts based on novel isoporous materials and fabrication techniques are discussed in the following sections.

3.2. Isoporous membranes

Isoporous membranes can be classified into two categories: lithography and non-lithography including anodization, track-etching, and self-assembly based methods. The characteristics of these membranes are summarised in Table 1, and their fabrication methods are described below.

3.2.1. Isoporous membranes by lithography

Lithography was originally developed for microelectronics manufacturing processes, and the method applies various UV and plasma etching steps through a patterned template to create semiconductor silicon chips with well-ordered and dense pore structures. This method can be applied to the fabrication of both polymeric and inorganic membranes with pore sizes from 0.5 to 50 μm which is within the microfiltration range (Nanoengineered et al., 2013). Bioseparation applications of these membranes focus on isolating and analysing circulating tumour cells (Zheng et al., 2007, Xu et al., 2010, Urabe et al., 2006). Their use has also been explored in facilitating cell culture imaging (Kim et al., 2014) and isolating plant organelles (Sabirova et al., 2020). However, expensive lithography-associated methods can currently only be commercialised at analytical scales and hence are only suitable for dealing with high-value and low-volume products. Moreover, the method currently makes only pore sizes within the range of microfiltration applications. The recovery of proteins and common viral vectors requires a finer pore within the ultrafiltration range.

Table 1
Current methods for fabricating isoporous membranes, their pore size range, pore density and their advantages and disadvantages. Information is adapted from: (Nanoengineered et al., 2013) and (Sabirova et al., 2020). The SEM pictures of membranes are reprinted with permission from (Osmanbeyoglu et al., 2009, Sabirova et al., 2020, Apel, 2001, Zhang et al., 2020)

Fabrication methods	Materials	Pore size	Pore density	Advantages & Disadvantages
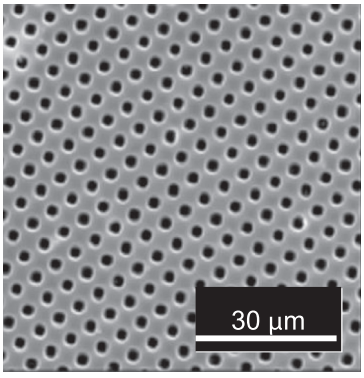 Lithography	Inorganic (e.g. Silicon, SiO_2, Si_3N_4, Metal) Organic (Polyimide, PET, PEGDA, SU-8, PDMS, Parylene, Mylar, Kapton)	5 nm - 1 mm	10^6 -10^{10} pore/cm^2	Excellent mechanical stability Chemical inertness Biocompatible Versatile material Good for mass production Expensive
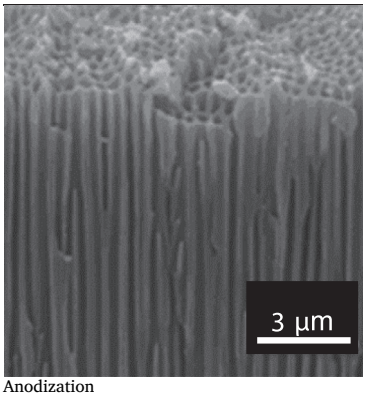 Anodization	Aluminium, Silicon, Titanium, Magnesium	5 nm -10 μm	10^9-10^{10} pore/cm^2	Less expensive Excellent mechanical stability Chemical inertness Biocompatible Brittleness Limited material choice Low permeability
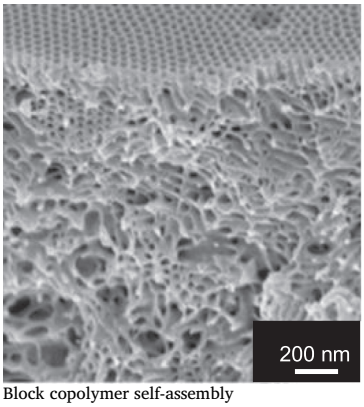 Block copolymer self-assembly	PS, PMMA, PLA, PVP, PI & CNTs based polymers	0.7 nm - 1 μm	10^{10} pore/cm^2	Promising mechanical stability via SNIPS Scalable for SNIPS Chemical inertness Biocompatible Various material choice High permeability Expensive
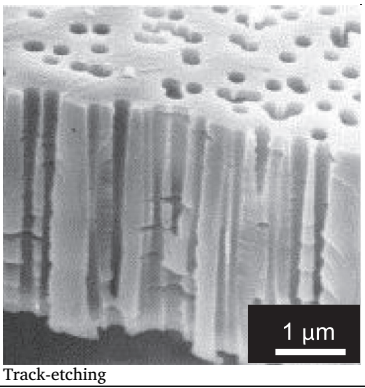 Track-etching	PET, PC, PP, PVDF, PI	10 nm - 3 μm	10^5-10^9 pore/cm^2	Excellent mechanical stability Biocompatible Chemical inertness Expensive Non for scalable production Low permeability

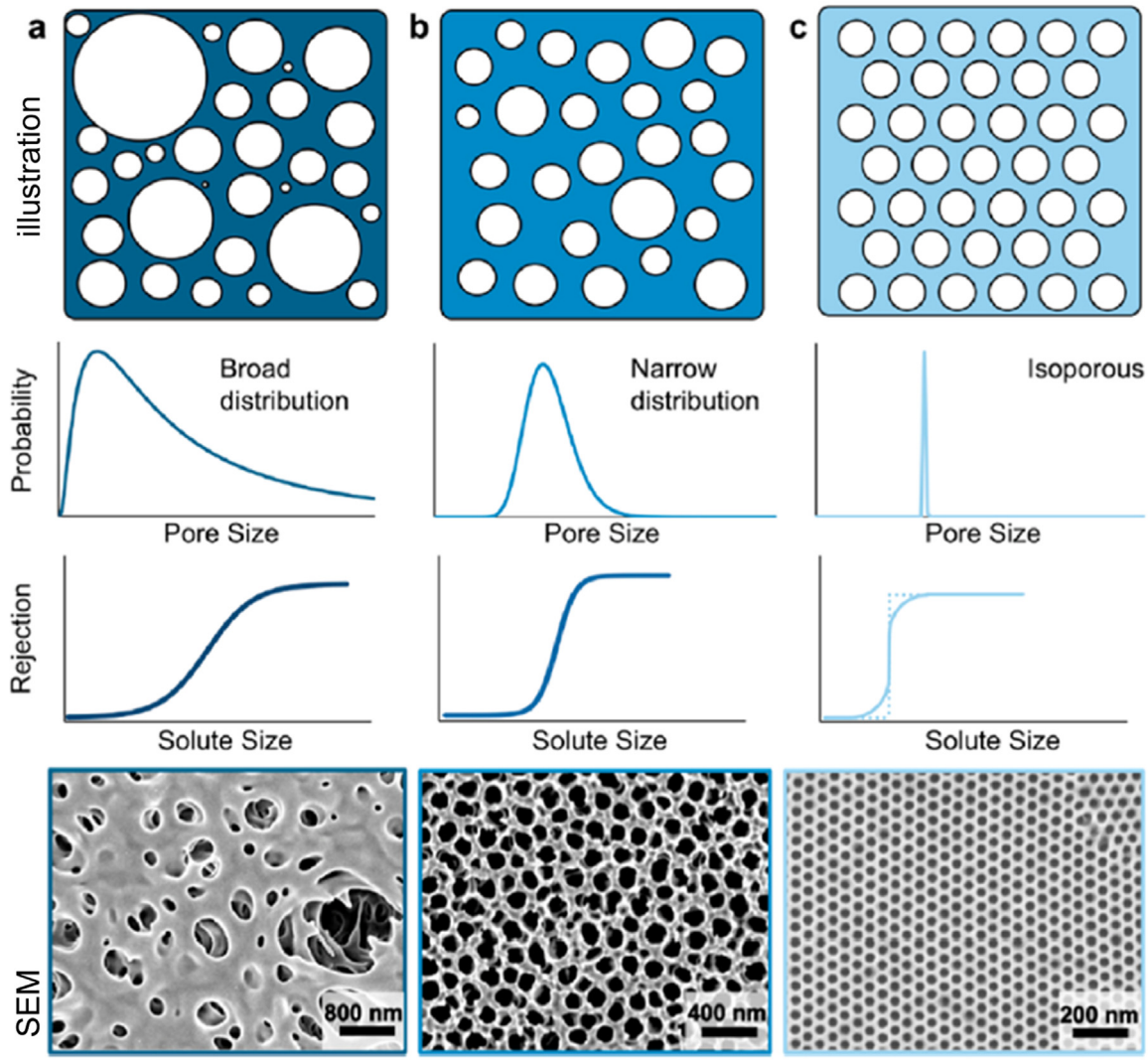

Fig. 5. (a) A model of commercially available polyethersulfone (PES) membrane made by NIPs. The pore size distribution and rejection profile are shown in the second and third rows, respectively. An example SEM image is shown in the fourth row. (b) An example of near isoporous membrane fabricated by an AAO membrane. (c) An ideal isoporous membrane (represented by the image of a section of block copolymer-derived AAO membrane) that shows the narrowest pore size distribution and highest pore density in the SEM image at a small scale. The figure is reprinted with permission from (Nanoengineered et al., 2013). Copyright 2021 Elsevier.

3.2.2. Track etched membranes

Track-etched membranes are mostly made of polycarbonate (PC) or polyethylene terephthalate (PET). They are prepared by high-energy particles or ions from a nuclear reactor or ion beams into the dense polymer films, followed by chemical etching steps for washing out any residuals (Ileri et al., 2013). These methods yield membranes with nearly identical pore sizes from 10 nm to several microns with straight pore channels. However, porosity is relatively low and pore size is not always identical due to the bombardment of ions forming overlapping tracks (Sabirova et al., 2020). Hence these membranes have good selectivity but limited permeability, which is not suitable for large-scale filtration. As the fabrication methods are relatively expensive, track-etched membranes are only commercially available at small scales with limited applications for laboratory filtration and cell culture (Apel, 2001).

3.2.3. Anodic aluminium oxide (AAO) membranes

Anodic aluminium oxide membranes have uniform pore sizes and are manufactured from 4 nm to 300 nm, covering the range for microfiltration and ultrafiltration (Hwang et al., 2002). The surface pore density is very high, and straight pore channels are throughout the cross section as an active separation layer. The fabrication of AAO membranes is first via a mild anodization step followed by a hard anodization step where a highly ordered pore structure is formed (Patel et al., 2020). Despite promising separation performance and extensive possible applications, AAO membranes are only available at analytical scales. The long cylinder pore channels in the selective layer through the membrane cross-section reduce the overall permeability (Hwang et al., 2002, Peng Lee and Mattia, 2013). The brittleness of AAO makes it challenging to integrate into a typical membrane filtration module or to be constructed as hollow fibres, which hinders the development of the membranes to production scales (Sharma and Bracewell, 2019). Moreover, it is difficult to manufacture defect-free AAO membranes at a large scale due to limitations of current fabrication techniques. The existence of defects has been reported in commercial AAO membranes (Peng Lee and Mattia, 2013).

3.2.4. Self-assembled block copolymer membranes

Block copolymers are macromolecules that consist of two or more blocks of repetitive units that are joined by covalent bonds (Bastakoti and Liu, 2017). The polymeric blocks are thermodynamically incompatible and can assemble into different patterns based on a series of factors, such as the percentage of the block (f_A), degree of polymerisation (N), the interaction between polymers and solvents (χ)

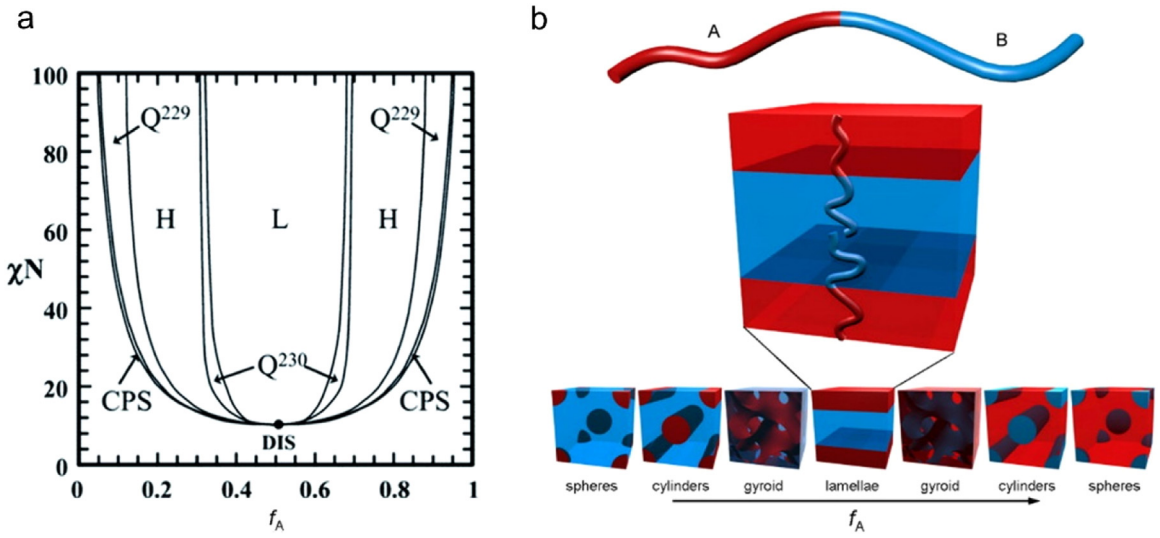

Fig. 6. (a) Theoretical simulation of phase diagram of diblock copolymer in melt. χ Flory-Huggins interaction, N the degree of polymerisation, f the fraction of one block. The figure is reprinted with permission from (Matsen and Bates, 1996, Khandpur et al., 1995). Copyright 1995 American Chemical Society. (b) A schematic phase diagram of diblock copolymer self-assembly in the melt. The figure is reprinted with permission from (Darling, 2007). Copyright 2007 Elsevier.

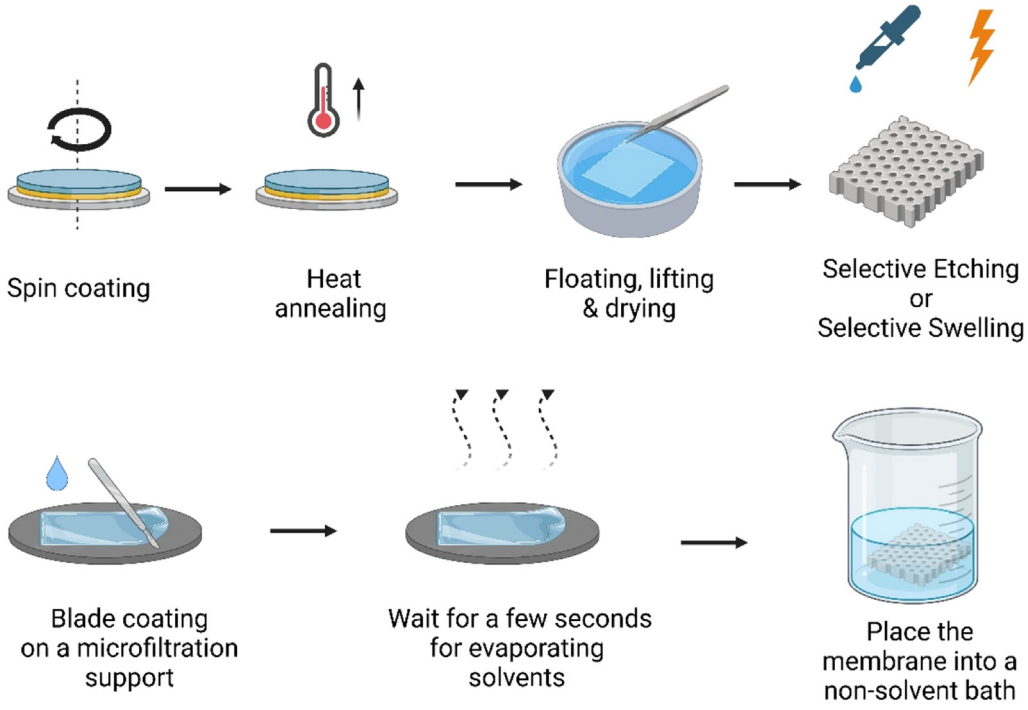

Fig. 7. The generic fabrication routes via selectively etching or swelling (top) and via SNIPS (bottom). The figure (top) is adapted from (Yang et al., 2006) and is created by Biorender (Aoki and BIORENDER, 2017).

(Bastakoti and Liu, 2017, Nie and Kumacheva, 2008). Among these patterns that are displayed in Fig. 6b, cylindrical structures are used for fabricating porous membranes for ultrafiltration purposes. Self-assembled block copolymers can be fabricated as isoporous membranes with uniform pore size, high porosity and straight pore channels. Compared with AAO membranes, block copolymer membranes are sufficiently flexible to be integrated into various modular filtration designs, such as flat sheets or hollow fibres (Hilke et al., 2013). Block copolymer membranes can also show stimuli responses such as to pH, which could be particularly suitable for protein separation because they charge differently at various pH conditions (Nunes et al., 2011).

As shown in Fig. 7, the fabrication of block copolymer membranes is performed by one of two pathways: (I) selective etching or swelling (II) self-assembly and non-solvent-induced phase separation (Nunes, 2020). The former normally goes through the coating, annealing, floating, and etching or swelling (Yang et al., 2006). This method makes thin film composite (TFC) membranes with a two-layer structure: a selective thin block copolymer layer on the top and a highly permeable backing layer that provides mechanical support for filtration applications.

The latter is abbreviated as SNIPS. The fabrication process involves two steps combining the features of block copolymer self-assembly and the well-known non-solvent-induced phase separation (NIPs) process pioneered by Loeb and Sourirajan (Loeb and Sourirajan, 1963). Firstly, a polymeric solution is cast onto a plate by blade coating, followed by vaporising solvents in the air when the block copolymer starts to assemble at the surface. Next, the sample is immersed in a non-solvent bath,

typically water. The non-solvent phase penetrates from the film surface and substitutes the original solvent underneath the skin layer where a macroporous supporting layer is formed. Apart from blade coating, dip coating and spray coating have also been used for fabricating polymeric membranes at different scales (Khan et al., 2014).

3.3. Locating isoporous membranes in the permeability-selectivity plot

Based on data published by Mehta and Zydney (Mehta and Zydney, 2005), an updated selectivity-permeability analysis including isoporous membranes is plotted in Fig. 8. Black symbols scattering at the conventional boundary are commercial membranes such as polysulfones, cellulosic and acrylic and acrylonitrile. The performance of block copolymer-based membranes (red symbols) via etching, swelling and SNIPS are widely spread out but remain within the conventional boundary. Overall, block copolymer membranes via swelling and etching provide better permeability, and the SNIPS method performs better in selectivity. Although the maximum separation factor of AAO membranes reaches around 90, the permeability is not very promising due to their thick active separation layer, which limits their throughput. Reducing the thickness of AAO discs can increase the permeability but decrease the mechanical strength and robustness, which tends to generate creaks and defects during manufacturing and applications.

Among these isoporous membranes, block copolymer membranes seem a promising candidate to overcome the trade-offs and towards the new boundary (green dashed line in Fig 8.) generated by simulation, based upon an isoporous membrane of fixed porosity and an active separation layer thickness of 1 μm^{-1} (Hampu et al., 2020). However, there are a few reasons why experimental data cannot match predictions. One important reason is that BSA (hydrodynamic radius, R_h ~ 4 nm) as the benchmark solute is too small for assessing the performance of current

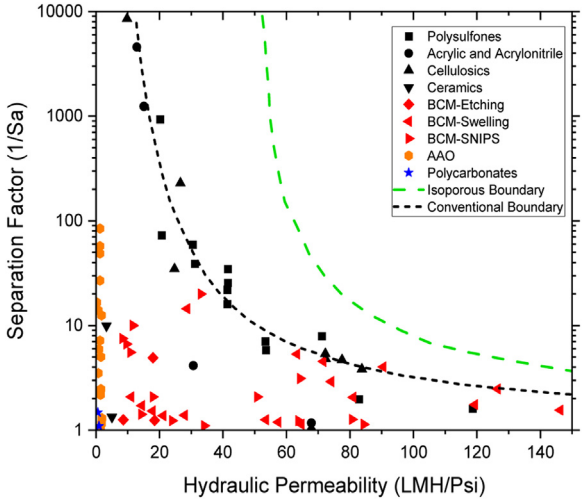

Fig. 8. The updated selectivity-permeability performance of isoporous ultrafiltration membrane candidates and commercial membranes by using BSA as a benchmark solute. The black dashed line and green dashed line follow a log-normal distribution and are generated by theoretical simulation with the assumption ($\varepsilon/\delta = 1\ \mu m^{-1}$) (Mochizuki and Zydney, 1993). The membrane performance data is extracted from (Mehta and Zydney, 2005, Lee and Mattia, 2013, Hampu et al., 2020)

block copolymer membranes because these membranes have an averagely larger pore size than commercial membranes.

The selectivity-permeability performance for filtrating PEO at 100 KDa (R_h ~ 10 nm) becomes significantly better than the results of BSA filtration, which indicates that block copolymer membranes could be

Table 2
A summary of recent ultrafiltration and sterile filtration applications of isoporous membranes for bioprocessing applications.

Year	Materials	Model solutes	Milestones	Ref.
2005	PS-b-PMMA	HRV14 (30nm)	Thin-film (pore size~15 nm, thickness~80 nm), was etched by hydrofluoric acid, and was coated on a commercial microfiltration membrane (pore size~0.2 μm, thickness~150 μm). Its selectivity was assessed by using the filtrate infecting HeLa cells, and was benchmarked with the performance with AAO and track-etched membranes	(Yang et al., 2006)
2007	PS-b-PMMA	HRV14 (30nm)	Thin-film (pore size~17 nm, thickness~160 nm), was etched by oxygen plasma, and crosslinked on a commercial microfiltration membrane (pore size~0.2 μm, thickness~150 μm). The filterability test is performed by using the feed and filtrate to infecting HeLa cells at different diluted concentrations.	(Yang et al., 2008)
2010	PS-b-PMMA	BSA/hGH	The pore size of PS-b-PMMA membranes was reduced to 6 nm by coating with a Au layer, which was used as a novel drug delivery system for in vitro delivering BSA and human growth hormone (hGH). A constant releasing rate of hGH in vivo for over 3 weeks was observed.	(Jackson and Hillmyer, 2010)
2013	PS-b-P4VP	BSA/IgG BSA/BHb	A 50 cm^2 isoporous membrane is fabricated via SNIPS with the toper layer (pore size ~34 nm, thickness 100 nm). The ultrafiltration was performed to separate BSA/IgG by size and BSA/BHb by surface charge. The selectivity for theformer achieved 87 at pH 7.4, and the selectivity achieved 10 at pH 4.7.	(Qiu et al., 2013)
2019	pGO-PS-b-P4VP	BSA/IgG	Polymer-grafted (pGO) nanosheets were grafted on PS-b-P4VP membranes via SNIPS with the top layer (pore size 25 nm, thickness 200 nm). Filtration experiments compare the performance of pGO-PS-b-P4VP membrane with PS-b-P4VP membrane for separation binary protein mixtures (BSA/IgG). The former performed better antifouling resistance with 66% enhanced flux and highest separation factors (33) in the record.	(Shevate et al., 2019)
2009	AAO	BSA/BHb	AAO membranes show high selectivity (>42) for separating between bovine serum albumin (BSA) and bovine hemoglobin (BHb).	(Osmanbeyoglu et al., 2009)
2014	AAO	Hepatitis c virus	The enrichment efficiency (infectivity percentage after unit operation) of ultrafiltration using AAO is over four times higher than conventional ultracentrifugation methods.	(Jeon et al., 2014)
2019	AAO	BSA/BSA nano particles	AAO has shown excellent fouling resistance and a 3-4 higher selectivity compared with a commercial polymer membrane.	(Sharma and Bracewell, 2019)
2006	AAO/ PC track etched	LNTs	AAO and polycarbonate track etched membranes are used to produce lipid nanotubes with customised diameters.	(Guo et al., 2006)
2016	PC track etched	LNTs	Extrusion through PC filters gave a 67.9% reduction in liposome size, which is highest among a few mainstream nanosizing methods.	(Ong et al., 2016)

Table 3
Spinout companies focusing on isoporous membranes for bio-separation applications.

Innovation	Company	Ref.
PS-b-P4VP di-block copolymer ultrafiltration membranes via SNIPS for virus clearance in monoclonal antibodies manufacturing process	Terapore (https://www.terapore.com/)	(Teraporetech Inc 2020)
Block copolymer nanofiltration membranes for water purification purposes	Anfiro (https://www.anfiro.com)	(Anfiro Inc 2020)
AAO isoporous membranes and templates for lab and biomedical research	Topmembranes (http://www.topmembrane.com/)	(Topmembrranes Technology 2022)
Silicon-based isoporous membrane for biomedical applications and material study	SiMPore (https://simpore.com/)	(Simpore Inc 2022)

more suitable for separating large particles, such as viral vectors and LNPs (Hampu et al., 2020). Another reason is that the porosity to active thickness ratio (ε/δ) of block copolymer membranes is generally low (0.2 to 1 μm^{-1}), compared with 1 μm^{-1} for commercial NIPS membranes (Mehta and Zydney, 2005)[53]. As their surface porosity is high enough, this indicates that block copolymer membranes have a thicker skin separation layer. Further research should address on controlling the thickness of the active layer in SNIPS methods, in addition to searching for suitable backing materials for depositing thin block copolymer layer in the swelling or etching methods (Hampu et al., 2020).

4. Perspectives on isoporous membranes for bioprocessing

Isoporous membranes with scalable and customisable advantages have promising futures for purifying emerging genomic medicines such as viral vectors and liposome nanoparticles. A number of bio-separation applications involving proteins, viruses and LNPs by using block copolymer membranes, AAO, and track etched membranes have been demonstrated in the laboratory, which is summarised in Table 2. AAO membranes can achieve excellent rejection based on size discrimination and exhibit superior antifouling resistance. Nevertheless, such membranes suffer from poor permeability, which is limited by the long cross-sectional pore channels. The brittleness characteristic of alumina oxide also makes it difficult to scale up and be integrated into filtration modules.

From the selectivity-permeability perspective, the performance of current self-assembled block copolymer membranes is comparable with commercial membranes for BSA separations. However, in the separation of larger particles, such as PEO-100 KDa, their performance is markedly superior (Hampu et al., 2020), which makes them a promising candidate in ultrafiltration operations for the harvest of large biological products. Besides the selectivity-permeability performance, block copolymer membranes exhibit a variety of promising properties by modifying or grafting functional groups on the membrane surface. These beneficial features span across a spectrum that includes enhanced antifouling and antibiofouling (Tripathi et al., 2013), improved size/charge based rejection (Zhang et al., 2020), and multiple stimuli-response behaviour (Clodt et al., 2013). Moreover, the fabrication of block copolymer-based membranes can be achieved in a wide range of coating methods, and integrated into various filtration modules such as hollow fibre and flat sheets. These characteristics have attracted a number of spin-out companies active in the domain of developing isoporous membranes for bioseparations, biomedical research and water purification purposes (see Table 3). Further applications of block copolymer materials can be customised into the membrane with a wide pore size range that passes large viral particles and LNPs in sterile filtration. This could greatly reduce any bioburden handled by chromatography columns. The stimuli-response feature of the block copolymer is particularly suitable for separating charged biomacromolecules by adjusting the solution pH and charge (Qiu et al., 2013).

Declaration of Competing Interest

The authors declare that they have no known competing financial interests or personal relationships that could have appeared to influence the work reported in this paper.

Data availability

Data will be made available on request.

Funding

KM acknowledges the Engineering and Physical Sciences Research Council (EPSRC) for funding via EPSRC-SFI the Centre for Doctoral Training in Advanced Characterisation of Materials, grant EP/S023259/1.

Acknowledgements

KM acknowledges the Engineering and Physical Sciences Research Council (EPSRC) for funding via EPSRC-SFI the Centre for Doctoral Training in Advanced Characterisation of Materials, grant EP/S023259/1. He is also grateful to UCL Department of Biochemical Engineering and Chemical Engineering for financial and facility support of his PhD study.

References

Anfiro Inc, (2020). anfiro.com (accessed February 20, 2020).
Aoki, S., BIORENDER, Biorender. (2017).
Apel, P., 2001. Track etching technique in membrane technology. Radiat. Meas. 34, 559–566. doi:10.1016/S1350-4487(01)00228-1.
Bastakoti, B.P., Liu, Z., 2017. Multifunctional polymeric micelles as therapeutic nanostructures: targeting, imaging, and triggered release. Nanostruct. Cancer Therapy doi:10.1016/B978-0-323-46144-3.00010-6.
Carugo, D., Bottaro, E., Owen, J., Stride, E., Nastruzzi, C., 2016. Liposome production by microfluidics: potential and limiting factors. Sci. Rep. 6, 1–15. doi:10.1038/srep25876.
Clodt, J.I., Filiz, V., Rangou, S., Buhr, K., Abetz, C., Höche, D., Hahn, J., Jung, A., Abetz, V., 2013. Double stimuli-responsive isoporous membranes via post-modification of ph-sensitive self-assembled diblock copolymer membranes. Adv. Funct. Mater. 23. doi:10.1002/adfm.201202015.
Darling, S.B., 2007. Directing the self-assembly of block copolymers. Progr. Polymer Sci. (Oxf.) 32, 1152–1204. doi:10.1016/j.progpolymsci.2007.05.004.
Dorin, R.M., Sai, H., Wiesner, U., 2014. Hierarchically porous materials from block copolymers. Chem. Mater. 26, 339–347. doi:10.1021/cm4024056.
Guo, Y., Yui, H., Minamikawa, H., Yang, B., Masuda, M., Ito, K., Shimizu, T., 2006. Dimension control of glycolipid nanotubes by successive use of vesicle extrusion and porous template. Chem. Mater. 18, 1577–1580. doi:10.1021/cm051980v.
Hampu, N., Werber, J.R., Chan, W.Y., Feinberg, E.C., Hillmyer, M.A., 2020. Next-generation ultrafiltration membranes enabled by block polymers. ACS Nano 14, 16446–16471. doi:10.1021/acsnano.0c07883.
Hilke, R., Pradeep, N., Madhavan, P., Vainio, U., Behzad, A.R., Sougrat, R., Nunes, S.P., Peinemann, K.V., 2013. Block copolymer hollow fiber membranes with catalytic activity and pH-response. ACS Appl. Mater. Interfaces 5, 7001–7006. doi:10.1021/am401163h.
Hwang, S.K., Jeong, S.H., Hwang, H.Y., Lee, O.J., Lee, K.H., 2002. Fabrication of highly ordered pore array in anodic aluminum oxide. Korean J. Chem. Eng. 19. doi:10.1007/BF02697158.
Ileri, N., Faller, R., Palazoglu, A., Létant, S.E., Tringe, J.W., Stroeve, P., 2013. Molecular transport of proteins through nanoporous membranes fabricated by interferometric lithography. Phys. Chem. Chem. Phys. 15, 965–971. doi:10.1039/c2cp43400h.
Jackson, E.A., Hillmyer, M.A., 2010. Nanoporous membranes derived from block copolymers: from drug delivery to water filtration. ACS Nano 4, 3548–3553. doi:10.1021/nn1014006.
Jeon, G., Jee, M., Yang, S.Y., Lee, B.Y., Jang, S.K., Kim, J.K., 2014. Hierarchically self-organized monolithic nanoporous membrane for excellent virus enrichment. ACS Appl. Mater. Interfaces 6, 1200–1206. doi:10.1021/am4049404.
Jousma, H., Talsma, H., Spies, F., Joosten, J.G.H., Junginger, H.E., Crommelin, D.J.A., 1987. Characterization of liposomes. The influence of extrusion of multilamellar vesicles through polycarbonate membranes on particle size, particle size distribution and number of bilayers. Int. J. Pharm. 35, 263–274. doi:10.1016/0378-5173(87)90139-6.

Jungbauer, A., 2013. Continuous downstream processing of biopharmaceuticals. Trends Biotechnol. 31, 479–492. doi:10.1016/j.tibtech.2013.05.011.
Khan, M.M., Filiz, V., Bengtson, G., Shishatskiy, S., Rahman, M., Abetz, V., 2014. Erratum to: Functionalized carbon nanotubes mixed matrix membranes of polymers of intrinsic microporosity for gas separation. Nanoscale Res. Lett. 9, 1–12. doi:10.1186/1556-276X-9-698.
Khandpur, A.K., Förster, S., Bates, F.S., Hamley, I.W., Ryan, A.J., Bras, W., Almdal, K., Mortensen, K., 1995. Polyisoprene-Polystyrene Diblock Copolymer phase diagram near the order-disorder transition. Macromolecules 28. doi:10.1021/ma00130a012.
Kim, M.Y., Li, D.J., Pham, L.K., Wong, B.G., Hui, E.E., 2014. Microfabrication of high-resolution porous membranes for cell culture. J. Memb. Sci. 452, 460–469. doi:10.1016/j.memsci.2013.11.034.
Lee, K.P., Mattia, D., 2013. Monolithic nanoporous alumina membranes for ultrafiltration applications: characterization, selectivity-permeability analysis and fouling studies. J. Memb. Sci. 435, 52–61. doi:10.1016/j.memsci.2013.01.051.
Loeb, S., Sourirajan, S., 1963. Sea water demineralization by means of an osmotic membrane. In: Saline Water Conversion-II Chapter 9, Advances in Chemistry, 38. ACS doi:10.1021/ba-1963-0038.
Lundstrom, K., 2003. Latest development in viral vectors for gene therapy. Trends Biotechnol. 21, 117–122. doi:10.1016/S0167-7799(02)00042-2.
Matsen, M.W., Bates, F.S., 1996. Unifying weak- and strong-segregation block copolymer theories. Macromolecules 29. doi:10.1021/ma951138i.
Maurer, N., Wong, K.F., Stark, H., Louie, L., McIntosh, D., Wong, T., Scherrer, P., Semple, S.C., Cullis, P.R., 2001. Spontaneous entrapment of polynucleotides upon electrostatic interaction with ethanol-destabilized cationic liposomes. Biophys. J. 80, 2310–2326. doi:10.1016/S0006-3495(01)76202-9.
Mehta, A., Zydney, A.L., 2005. Permeability and selectivity analysis for ultrafiltration membranes. J. Memb. Sci. 249, 245–249. doi:10.1016/j.memsci.2004.09.040.
Mochizuki, S., Zydney, A.L., 1993. Theoretical analysis of pore size distribution effects on membrane transport. J. Memb. Sci. 82. doi:10.1016/0376-7388(93)85186-Z.
Nanoengineered, I.M., Warkiani, M.E., Bhagat, A.A.S., Khoo, B.L., Han, J., Lim, C.T., Isoporous Micro/Nanoengineered Membranes, (2013) 1882–1904.
Nie, Z., Kumacheva, E., 2008. Patterning surfaces with functional polymers. Nat. Mater. 7. doi:10.1038/nmat2109.
Nunes, S.P., Behzad, A.R., Hooghan, B., Sougrat, R., Karunakaran, M., Pradeep, N., Vainio, U., Peinemann, K.V., 2011. Switchable pH-responsive polymeric membranes prepared via block copolymer micelle assembly. ACS Nano 5, 3516–3522. doi:10.1021/nn200484v.
Nunes, S.P., 2020. Block Copolymer Membranes. In: Sustainable Nanoscale Engineering from Materials Design to Chemical Processing. Elsevier Inc., pp. 297–316. doi:10.1016/B978-0-12-814681-1.00011-4.
Ong, S.G.M., Chitneni, M., Lee, K.S., Ming, L.C., Yuen, K.H., 2016. Evaluation of extrusion technique for nanosizing liposomes. Pharmaceutics 8, 1–12. doi:10.3390/pharmaceutics8040036.
Osmanbeyoglu, H.U., Hur, T.B., Kim, H.K., 2009. Thin alumina nanoporous membranes for similar size biomolecule separation. J. Memb. Sci. 343, 1–6. doi:10.1016/j.memsci.2009.07.027.
Ozdilek, A., Avci, F.Y., 2022. Glycosylation as a key parameter in the design of nucleic acid vaccines. Curr. Opin. Struct. Biol. 73. doi:10.1016/j.sbi.2022.102348.
Patel, Y., Janusas, G., Palevicius, A., Vilkauskas, A., 2020. Development of nanoporous AAO membrane for nano filtration using the acoustophoresis method. Sensors (Switzerland) 20, 1–26. doi:10.3390/s20143833.
Peng Lee, K., Mattia, D., 2013. Monolithic nanoporous alumina membranes for ultrafiltration applications: Characterization, selectivity-permeability analysis and fouling studies. J. Memb. Sci. 435, 52–61. doi:10.1016/j.memsci.2013.01.051.
Phillip, W.A., Hillmyer, M.A., Cussler, E.L., 2010. Cylinder orientation mechanism in block copolymer thin films upon solvent evaporation. Macromolecules 43, 7763–7770. doi:10.1021/ma1012946.
Phillip, W.A., Mika Dorin, R., Werner, J., Hoek, E.M.V., Wiesner, U., Elimelech, M., 2011. Tuning structure and properties of graded triblock terpolymer-based mesoporous and hybrid films. Nano Lett. 11, 2892–2900. doi:10.1021/nl2013554.
Qiu, X., Yu, H., Karunakaran, M., Pradeep, N., Nunes, S.P., Peinemann, K.V., 2013. Selective separation of similarly sized proteins with tunable nanoporous block copolymer membranes. ACS Nano 7, 768–776. doi:10.1021/nn305073e.
Qiu, X., Yu, H., Karunakaran, M., Pradeep, N., Nunes, S.P., Peinemann, K.V., 2013. Selective separation of similarly sized proteins with tunable nanoporous block copolymer membranes. ACS Nano doi:10.1021/nn305073e.
Radjabian, M., Abetz, V., 2015. Tailored pore sizes in integral asymmetric membranes formed by blends of block copolymers. Adv. Mater. 27, 352–355. doi:10.1002/adma.201404309.
Robeson, L.M., 2008. The upper bound revisited. J. Memb. Sci. 320, 390–400. doi:10.1016/j.memsci.2008.04.030.
Sabirova, A., Pisig, F., Rayapuram, N., Hirt, H., Nunes, S.P., 2020. Nanofabrication of Isoporous membranes for cell fractionation. Sci. Rep. 10, 1–9. doi:10.1038/s41598-020-62937-5.
Sablani, S., Goosen, M., Al-Belushi, R., Wilf, M., 2001. Concentration polarization in ultrafiltration and reverse osmosis: a critical review. Desalination 141. doi:10.1016/S0011-9164(01)85005-0.
Samaridou, E., Heyes, J., Lutwyche, P., 2020. Lipid nanoparticles for nucleic acid delivery: current perspectives. Adv. Drug. Deliv. Rev. 154–155. doi:10.1016/j.addr.2020.06.002.
Segura, M.M., Kamen, A.A., Garnier, A., 2011. Overview of current scalable methods for purification of viral vectors. Methods Mol. Biol. doi:10.1007/978-1-61779-095-9_4.
Sharma, A., Bracewell, D.G., 2019. Characterisation of porous anodic alumina membranes for ultrafiltration of protein nanoparticles as a size mimic of virus particles. J. Memb. Sci. 580, 77–91. doi:10.1016/j.memsci.2019.02.071.
Shevate, R., Kumar, M., Cheng, H., Hong, P.Y., Behzad, A.R., Anjum, D., Peinemann, K.V., 2019. Rapid size-based protein discrimination inside hybrid isoporous membranes. ACS Appl. Mater. Interfaces 11, 8507–8516. doi:10.1021/acsami.8b20802.
Simpore Inc, (2022). https://simpore.com/(accessed September 1, 2022).
Singh, N., Heldt, C.L., 2022. Challenges in downstream purification of gene therapy viral vectors. Curr. Opin. Chem. Eng. 35. doi:10.1016/j.coche.2021.100780.
Srivastava, A., Mallela, K.M.G., Deorkar, N., Brophy, G., 2021. Manufacturing challenges and rational formulation development for AAV viral vectors. J. Pharm. Sci. 000. doi:10.1016/j.xphs.2021.03.024.
Teraporetech Inc., (2020). Teraporetech.com (accessed February 20, 2020).
Topmembrranes Technology, (2022). http://www.topmembrane.com/(accessed September 1, 2022).
Tripathi, B.P., Dubey, N.C., Choudhury, S., Simon, F., Stamm, M., 2013. Antifouling and antibiofouling pH responsive block copolymer based membranes by selective surface modification. J. Mater. Chem. B 1. doi:10.1039/c3tb20386g.
Urabe, M., Xin, K.Q., Obara, Y., Nakakura, T., Mizukami, H., Kume, A., Okuda, K., Ozawa, K., 2006. Removal of empty capsids from type 1 adeno-associated virus vector stocks by anion-exchange chromatography potentiates transgene expression. Mol. Therapy 13, 823–828. doi:10.1016/j.ymthe.2005.11.024.
Vishali, S., Kavitha, E., 2021. Application of membrane-based hybrid process on paint industry wastewater treatment. In: Membrane-Based Hybrid Processes for Wastewater Treatment doi:10.1016/B978-0-12-823804-2.00016-1.
Wang, J., Liu, Y., Liu, T., Xu, X., Hu, Y., 2020. Improving the perm-selectivity and antifouling property of UF membrane through the micro-phase separation of PSf-b-PEG block copolymers. J. Memb. Sci. 599, 117851. doi:10.1016/j.memsci.2020.117851.
Werber, J.R., Osuji, C.O., Elimelech, M., 2016. Materials for next-generation desalination and water purification membranes. Nat. Rev. Mater. 1. doi:10.1038/natrevmats.2016.18.
Xu, T., Lu, B., Tai, Y.C., Goldkorn, A., 2010. A cancer detection platform which measures telomerase activity from live circulating tumor cells captured on a microfilter. Cancer Res. 70, 6420–6426. doi:10.1158/0008-5472.CAN-10-0686.
Yang, Z., Zhang, Z., 2018. Engineering strategies for enhanced production of protein and bio-products in Pichia pastoris: a review. Biotechnol. Adv. 36, 182–195. doi:10.1016/j.biotechadv.2017.11.002.
Yang, S., Ryu, I., Kim, H.Y., Kim, J.K., Jang, S.K., Russell, T.P., 2006. Nanoporous membranes with ultrahigh selectivity and flux for the filtration of viruses. Adv. Mater. 18, 709–712. doi:10.1002/adma.200501500.
Yang, S., Park, J., Yoon, J., Ree, M., Jang, S.K., Kim, J.K., 2008. Virus filtration membranes prepared from nanoporous block copolymers with good dimensional stability under high pressures and excellent solvent resistance. Adv. Funct. Mater. 18, 1371–1377. doi:10.1002/adfm.200700832.
Zhang, Y., Almodovar-Arbelo, N.E., Weidman, J.L., Corti, D.S., Boudouris, B.W., Phillip, W.A., 2018. Fit-for-purpose block polymer membranes molecularly engineered for water treatment. NPJ Clean Water 1, 1–14. doi:10.1038/s41545-018-0002-1.
Zhang, Z., Rahman, M.M., Abetz, C., Höhme, A.L., Sperling, E., Abetz, V., 2020. Chemically tailored multifunctional asymmetric Isoporous triblock terpolymer membranes for selective transport. Adv. Mater. 32. doi:10.1002/adma.201907014.
Zheng, S., Lin, H., Liu, J.Q., Balic, M., Datar, R., Cote, R.J., Tai, Y.C., 2007. Membrane microfilter device for selective capture, electrolysis and genomic analysis of human circulating tumor cells. J. Chromatogr. A 1162, 154–161. doi:10.1016/j.chroma.2007.05.064.